A Study of Carbon Nanotubes/Biodegradable Plastic Polylactic Acid Composites

Wei-Ming Chiu,[1] You-An Chang,[1] Hsan-Yuan Kuo,[1] Meng-Hung Lin,[2] Hua-Chiang Wen[3]

[1]*Department of Chemical and Materials Engineering, National Chin-Yi University of Technology, Taichung 41111, Taiwan, Republic of China*
[2]*Department of Mechanical Engineering, National Chin-Yi University of Technology, Taichung 41111, Taiwan, Republic of China*
[3]*Institute and Department of Mechanical Engineering, National Chiao Tung University, Hsinchu 30010, Taiwan, Republic of China*

Received 20 October 2006; accepted 2 December 2007
DOI 10.1002/app.27796
Published online 27 February 2008 in Wiley InterScience (www.interscience.wiley.com).

ABSTRACT: Fabrication process was successfully used to embed carbon nanotubes (CNTs) in a polylactic acid (PLA) matrix, forming a composite nanostructure. For the composites, nanoindentation is often used to characterize their mechanical properties (e.g., hardness and Young's moduli). In this experiment, the varied concentrations of CNTs in PLA were analyzed in their mechanical performance. The distribution and conformation of CNTs in the PLA were studied by X-ray diffraction. Then, electrical characterization was performed by four-probe method. Thermal properties were checked by TGA and DSC. Furthermore, the CNTs/PLA nanocomposites were observed by SEM. According to the experimental result, purified CNTs showed better dispersing and properties in the CNTs PLA nanocomposites. © 2008 Wiley Periodicals, Inc. J Appl Polym Sci 108: 3024–3030, 2008

Key words: carbon nanotubes; polylactic acid; nanocomposite; nanoindentation

INTRODUCTION

Carbon nanotubes (CNTs) have high elastic module, approaching 1 TPa, and exceptional tensile strengths, ranging from 20 to 100 GPa. The transference of these properties into the corresponding mechanical properties in actual composites depends on many other *in situ* features. Also, CNTs have attracted other applications in electronic devices[1] and sensors[2] due to their good electrical and chemical properties. Nevertheless, controlled-release biodegradable nanoparticles can be made from a polylactic acid (PLA). PLA and its copolymer PLGA are common biocompatible polymers that are used for making nanoparticles. Furthermore, biodegradable PLA, because of many carboxyl groups,[3] is one of the promising candidates for supplying inducers for the bone-like apatite nucleation.[4,5] A carboxyl group is known to induce apatite nucleation and can be formed by hydrolyzation of PLA.[6,7]

The mastering of CNTs for composite applications depends on strength characterization studies that relate the dependence of indentation to the CNTs of surface. Carbon nanotube-based polymer nanocomposites are attractive because of their improved mechanical,[8,9] electrical,[10–13] and thermal properties. Initial crystallization studies on well-dispersed samples in copolymers show that tubes act as a nucleating agent for nanocomposite. The polymer composites are also studied for aligned CNTs samples.[14,15]

In this article, the fabrication process was used successfully to embed multiwalled carbon nanotubes (MWCNTs) in a PLA matrix, forming composite nanostructure. Additionally, the CNTs were also purified by a mixture of 98% sulfuric acid and 70% nitric acid in the proportion of 3 : 1 (volume : volume) to remove the transition metal catalyst, amorphous carbon and graphitic nanoparticle. The well-dispersed CNTs in thin PLA film were fabricated. Nanoindentation introduced controlled cracks and the damage behavior to examine the inner composite property. These hallmarks of CNTs/PLA matrix interface exhibit by a Berkovich indenter. The quantitative indentation data is used to determine the CNTs/PLA matrix, thus, the axial modulus was studied. Further, the morphology, electrical and thermal properties of the CNTs/PLA nanocomposites were also observed in this study.

EXPERIMENTAL

Preparation of polylactic acid nanocomposite materials

First, MWCNTs : CNTs (Mingxin Technology, Taipei, Taiwan; purity: tube diameter: 8–15 nm, length:

Correspondence to: W.-M. Chiu (cwm@mail.ncut.edu.tw).
Contract grant sponsor: National Science Council of Taiwan.

50 μm) were mixed with 98% sulfuric acid and 70% nitric acid at 50°C under ultrasonic vibration. Next, CNTs and acid solvent were separated from those acid solutions through a Teflon filter film (mesh: 0.5 μm). After that, the filtered CNTs were rinsed with deionized water until the pH reaches about 6. Finally, the CNTs were heated to 100°C in an oven for 24 h to remove surplus water.

Further, the solution blending method is used to prepare two kinds of lactic acid nanocomposite materials, namely PLA (Wei-Mon Industry; purity: expansible)/nonpurified or purified CNTs. As far as the solution matrix is concerned, the polar solvent demonstrates better dispersion effect on CNTs before and after purification. Especially, because of the presence of a larger functional base COOH on the surface of the purified CNTs, it has more obvious dispersion effect. Therefore, strong polar solvent (tetrahydrofuran, THF) can be used. In this experiment, different proportions of CNTs were added into THF, mixed them with PLA solution and finally placed them into a vacuum oven to remove the solvent. The varied concentrations of CNTs in PLA were 1, 3, 5, and 7%. The obtained nanocomposite material is made into specimens by the thermal compression method.

Experimental analysis

The crystalline structure and crystallographic orientation of CNTs/PLA nanocomposites were determined using grazing incident angle X-ray diffraction (XRD) (PANalytical X′ Pert PRO). The power of XRD (Cu Kα radiation) was fixed at 45 kV and 40 mA. The incident angle of X-ray was fixed at 0.5°. To compare the diffraction intensities of different samples, the XRD angles (2θ) spanned from 30° to 60°. For the nanocomposites, nanoindentation is often used to characterize their hardness and Young's moduli. Thus, mechanical properties of CNTs/PLA nanocomposites were characterized by a Nano Indenter XP (MTS Cooperation, Nano Instruments Innovation Center, Oak Ridge, TN) using a diamond Berkovich indenter tip (tip radius ~ 50 nm). We followed the continuous contact stiffness measurement (CSM) procedure, which was accomplished by superimposing small oscillations at 75 Hz on the force signal to measure displacement responses. Electrical property was determined by a conductance meter. The four-probe (Verbeing SR-4, Keithley Source Meter Model 2400) contacts the sample during the measurement, with a supplied voltage of 2.1 V DC. The measured current value A with the probe determines the surface resistance (Rs) of the samples. The thermogravimetry (TGA) analyzer used in this study was a Thermal Advantage Software, TA Instruments, TGA Q-500. Sample was burned in nitrogen and air environment, respectively, at a temperature from 50 to 800°C with an increment of 10°C/min. The differential scanning calorimetry (DSC) used in this study was a TA Instruments, DSC 2010. The testing temperature was 25–115°C with an increment of 10°C/min in nitrogen environment. The scanning electron microscope (SEM), model: JEOL-JSM-6360/LV, is mainly used to observe the dispersion of CNTs before and after purification, as well as the morphological change between the CNTs and PLA. The specimen surface was sputtered with gold. The distance of specimen to detector was 15 mm in the SEM observation.

RESULTS AND DISCUSSION

The PLA is available as a novel material within grafting nanoscale size of CNTs. It is believed that adding CNTs to PLA will induce a change in physical property, thus it can serve as a high suitable scaffold for cartilage, as well as a bone in the field of tissue engineering. Also, the unique structure of the CNTs/PLA matrix is expected to provide nanoscale perfection. Hence, it can be concluded that the CNTs inside PLA is achieved as cell-friendly for biomaterials with good mechanical property.

Further, how to reveal the aligned tube direction polymer crystals arrange themselves in PLA matrix is suggested. To fabricate the lamellar parallel to tube axis, CNTs act as a nucleating agent for PLA, chains grow parallel to the draw direction. This observation is interesting because oriented tubes can be used as a template to orient polymer crystals.

X-ray diffraction spectra

Figure 1 features the XRD spectra of CNTs/PLA nanocomposites with the varied concentration of CNTs in PLA (1, 3, 5, and 7%). The CNTs/PLA film featured an amorphous peak with similar intensities and greater full width at half maximum (FWHM). A strong and wide diffraction peak of PLA with amorphous carbon was observed from 10° to 20°. Also, the spectrum for 7% indicates the phosphorous element (29.5°), which is induced by the dispersed solution. Because of the initial solution blending method, some the lactic acid nanocomposite may get contaminated. And, it is suggested that phosphorous element may be present irrespective by solution blending method. Further, the nonpurified CNTs/PLA and purified CNTs/PLA composites show nearly the same behavior in XRD spectra in this study.

Nanoindentation

The modulus of 1, 3, 5, and 7% CNTs/PLA matrix were measured directly via a diamond Berkovich

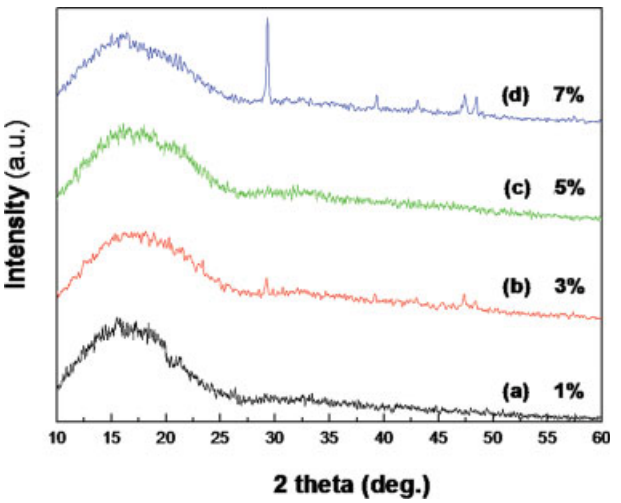

Figure 1 Features the X-ray diffraction spectra of CNTs/PLA nanocomposites with the variation of concentration of CNTs in PLA (1, 3, 5, and 7%). [Color figure can be viewed in the online issue, which is available at www.interscience.wiley.com.]

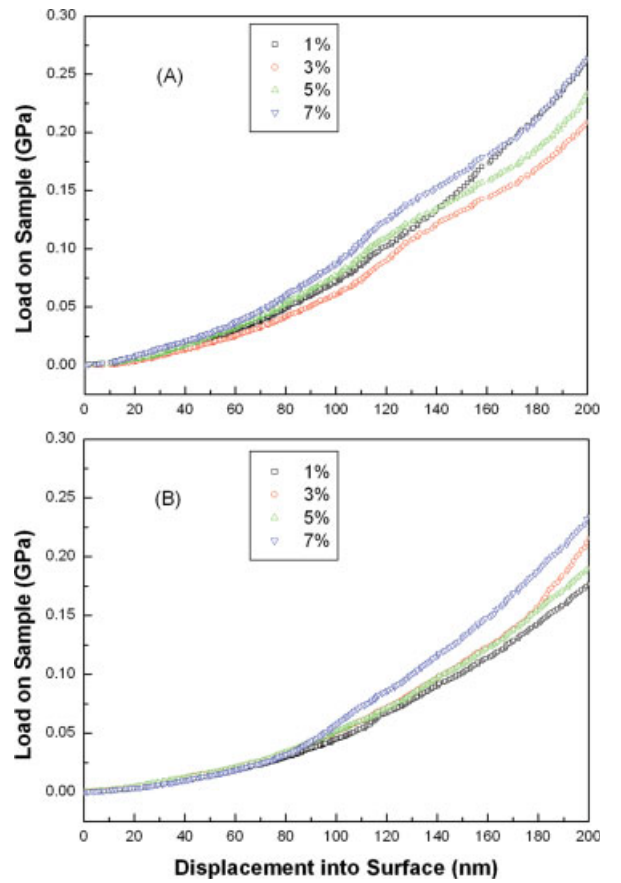

Figure 2 The force load and measuring obtained the load-deformation curve. Those curves were derived from the load-deformation curve of CNTs/PLA composites with the variation of concentration of nonpurified (A) and purified (B) CNTs in PLA (1, 3, 5, and 7%). [Color figure can be viewed in the online issue, which is available at www.interscience.wiley.com.]

indenter tip. Applying a force load provided the load-deformation curve. Those curves were derived from the load-deformation curve using the specific area of the samples to obtain the initial modulus, as shown in Figure 2. By CSM procedure, this was accomplished by superimposing small oscillations at 75 Hz on the force signal to measure the displacement responses. The load-displacement curve was utilized to determine the Young's modulus and hardness. The mechanical scattering response depended on the film of the matrix and increased with the CNTs concentration. A homogeneous hybrid is obtained within both components, which are used to get a good interpenetration at the molecular scale.

Figure 3 plots the increase in modulus as a function of tip displacement. Thus, the elastic modulus increased with increasing the concentration of CNTs. This evidenced that the CNTs effectively strengthen the composites embedded into PLA. Figure 4 also plots the hardness of CNTs/PLA films on the various CNT contents. The hardness value increased with increasing the amount of CNTs. The cause of increasing Young's modulus and hardness with CNTs content is due to the good dispersion of CNTs in the PLA matrix. The results revealed that the CNTs reinforced effectively the mechanical strength of PLA. Compared with the nonpurified CNTs/PLA

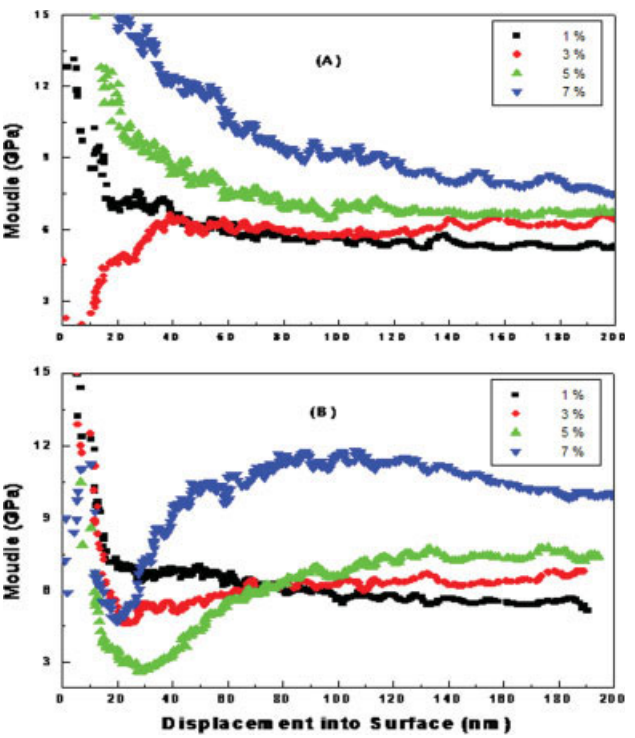

Figure 3 Plots of the increased modulus compared with a tip displacement. Thus, the elastic modulus increased with increasing the content of nonpurified (A) and purified (B) CNTs supply. [Color figure can be viewed in the online issue, which is available at www.interscience.wiley.com.]

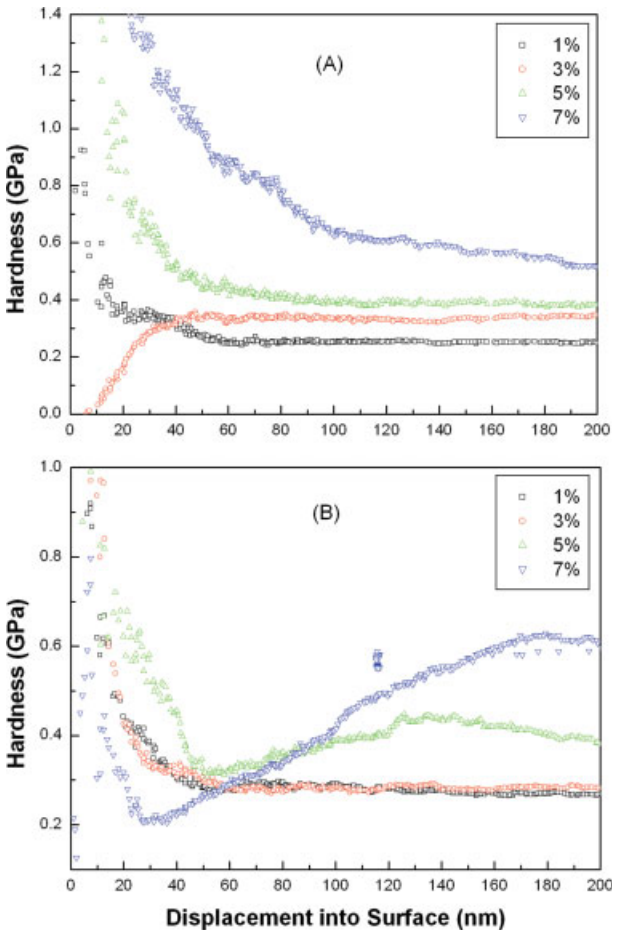

Figure 4 Plots of the hardness of CNTs/PLA nanocomposites with various CNTs contents. The hardness value increased based on the number of nonpurified (A) and purified (B) CNTs. [Color figure can be viewed in the online issue, which is available at www.interscience.wiley.com.]

composites, the mechanical property of purified CNTs/PLA composites are better.

Based on the comparison of each figure, under the same testing conditions, mechanical property of CNTs/PLA composites showed a more significant increase than that of pure PLA, and improved a lot with the increasing amount. It was expressed as the virtue that a repulsion of dipole force is generated by the polar functional groups of the CNTs. Then, the purified CNTs increase the dispersion of CNTs in the polymer free volume. On the other hand, hydrogen and little covalent bonding between PLA and CNTs could be created after a purified CNTs process. Our studies reveal that the mechanical behaviors of CNTs/PLA composites can be significantly improved as summarized in Table I.

The surface resistivity

Table II indicates the surface resistance of nanocomposites after the addition of purified CNTs. In this table, when 1% purified CNT is added, the composites surface resistivity decreases to 2.33×10^8 Ωm, and after 7% is added, surface resistivity decreases to 6.19×10^5 Ωm. Comparison of PLA matrix with nonpurified and purified CNTs, after adding 3% nonpurified CNTs is added, show that the surface resistance of the composite decreases significantly, mainly because, after purification, there are polar functional groups on the CNTs surface, and as compared with nonpurified CNTs, purified CNTs are easy to disperse in polar solvents to avoid agglomeration of a large quantity of CNTs and formation of wider conduction distribution.

The thermal properties

Figure 5 shows the thermal decomposed behavior of CNTs/PLA composites. TGA curves were obtained by the analysis of PLA with different proportions of purified and nonpurified in nitrogen environment. In comparison with the difference of thermal stability of PLA before and after the addition at the same proportion of purified CNTs, the decomposed temperature of purified CNTs increases by 10°C as compared with nonpurified CNTs under identical conditions. This is because the purified CNTs can enhance the attraction and interface effect in the PLA matrix.

Figure 6 indicates the glass transition temperature (T_g) of the composite material of CNTs/PLA prepared with nonpurified CNTs and purified CNTs under different adding amounts of CNTs. In this experiment, heating test was carried out by using DSC to prepare the CNTs/PLA composites and

TABLE I
The Modulus and Hardness Properties of Nonpurified and Purified CNTs/PLA Nanocomposites were Characterized by Nano Indenter

Nonpurified CNTs content (%)	Modulus (Gpa)	Hardness (GPa)	Purified CNTs content (%)	Modulus (Gpa)	Hardness (GPa)
1	5.32	0.22	1	5.82	0.22
3	5.74	0.33	3	6.15	0.26
5	5.97	0.34	5	6.45	0.39
7	6.43	0.41	7	8.23	0.48

TABLE II
The Surface Resistance of Nonpurified and Purified CNTs/PLA Nanocomposites with Different Proportion

Nonpurified CNTs content (%)	Surface resistance (Ωm)	Purified CNTs content (%)	Surface resistance (Ωm)
0	1.00×10^{16}	0	1.00×10^{16}
1	1.46×10^{10}	1	2.33×10^{8}
3	3.75×10^{8}	3	4.52×10^{6}
5	4.29×10^{7}	5	8.33×10^{5}
7	2.30×10^{7}	7	6.19×10^{5}

observe the change in the glass transition temperature (T_g). According to this figure, for the composite material of CNTs/PLA after being reinforced by the addition of nonpurified CNTs, its T_g was 5–7°C higher than that of pure PLA polymer, and CNTs were filled into the PLA matrix in a dispersive manner. According to Zhang et al.,[16] first, the use of nanosize CNTs is similar in effect to a crosslinking agent: intermolecular friction increased and the movement of macromolecular chains was restricted. Second, the decrease in free volume of the matrix accelerates phase separation and limits the motion of some molecular chains so that the damping decreases. This figure shows that, after CNTs are filled into the free volume of polymer as the filler, there is not enough space between macromolecules for the adjustment of molecular chains, and T_g point will increase due to the increase in the addition of CNTs. In other words, the purified CNTs can increase more obviously the glass transition temperature of the composite material than that of nonpurified CNTs, because the purified CNTs can improve

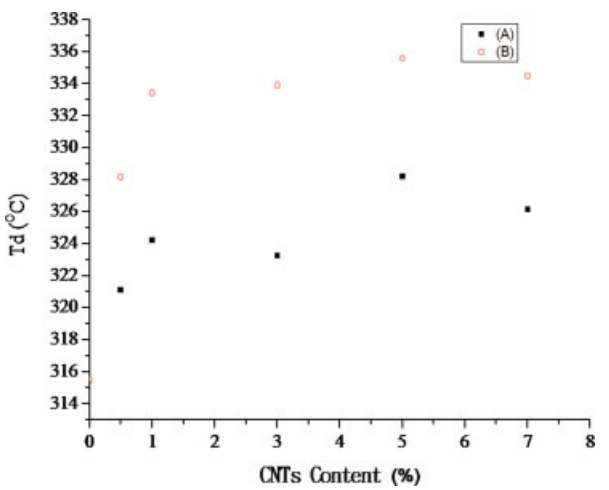

Figure 5 Trend figure of different contents of nonpurified (A) and purified (B) CNTs in CNTs/PLA nanocomposites versus thermal decomposed temperature. [Color figure can be viewed in the online issue, which is available at www.interscience.wiley.com.]

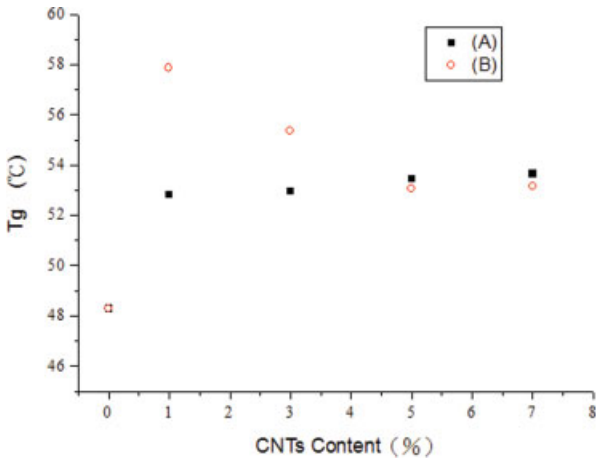

Figure 6 Trend of different contents of nonpurified (A) and purified (B) CNTs in CNTs/PLA composites versus glass transition temperature. [Color figure can be viewed in the online issue, which is available at www.interscience.wiley.com.]

the compatibility with PLA and achieve more uniform dispersion in PLA, so the improvement of T_g in purified CNTs/PLA composites is quite obvious.

The morphology of CNTs/PLA nanocompostites

In Figures 7 and 8, the interfaces between CNTs and matrixes can be observed. Before purification, the surface of CNTs takes on a complete structure, without any functional groups, so they are not easy to combine with matrixes, causing the matrixes unable to transfer the damaged force to CNTs under an external force. Therefore, through morphological observation, it is easily found that the surface of fracture is smooth or there are some holes on it, which are caused by poor combination between CNTs and PLA. After purification, some functional groups are formed on the surface of CNTs, which can combine with matrixes to some extent. Hence, the stress can be transferred to CNTs, and cause the pull-out of CNTs attached to PLA and irregular shape on the surface of fracture, indicating that there is a better interface effect between CNTs and PLA. However, in the SEM image of the CNTs/PLA composites, it seemed that the CNTs were damaged and its average length is shorter than that of original CNTs (50 μm).

CONCLUSION

In this study, a fabrication process was successfully developed to embed nonpurified and purified CNTs in PLA matrix.

According to this experimental result, the elastic modulus and the hardness for CNTs increased significantly. Further, according to the SEM image of

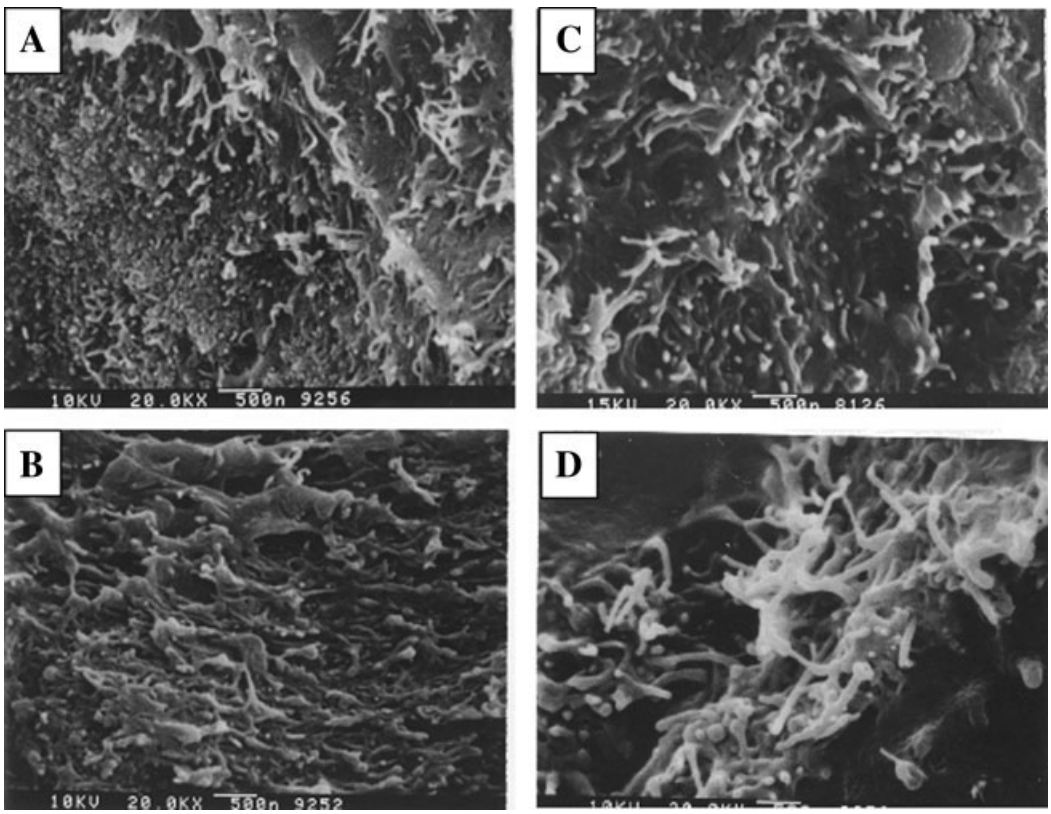

Figure 7 SEM analysis drawing of CNTs/PLA composites, under (20K) multiple, observe the morphological change in addition of nonpurified CNTs (A) 1%, (B) 3%, (C) 5%, and (D) 7%.

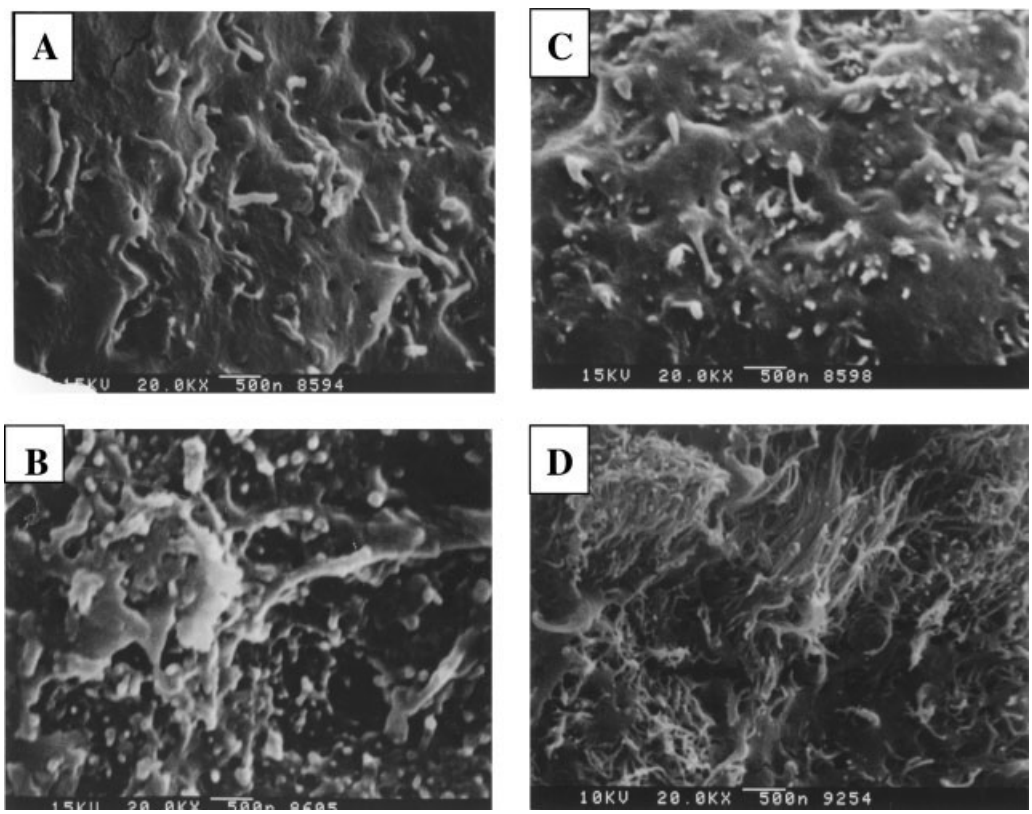

Figure 8 SEM analysis drawing of CNTs/PLA composites, under (20K) multiple, observe the morphological change in addition of purified CNTs (A) 1%, (B) 3%, (C) 5%, and (D) 7%.

CNTs/PLA nanocomposites, purified CNTs can achieve better effect upon dispersing it in the free volume of PLA material. Therefore, purified CNTs/PLA nanocomposites showed better mechanical properties and thermal stability.

The surface resistivity decreases upon adding about 1–7 CNTs. When nonpurified CNTs are added, surface resistivity of CNTs/PLA nanocomposites reduce from 1×10^{16} to 2.30×10^{10} Ωm. At the same condition, addition of purified CNTs will cause the surface resistivity of CNTs/PLA nanocomposites decrease to 6.19×10^{8} Ωm.

However, the nonpurified CNTs/PLA and purified CNTs/PLA composites show essentially the same behavior in the XRD spectra.

Technical support from the National Nano Device Laboratories (NDL-95S-C-067) and Plastics Industry Development Center are acknowledged.

References

1. Tans, S. J.; Verschueren, A. R. M.; Dekker, C. Nature 1998, 393, 49.
2. Kong, J.; Franklin, N. R.; Zhou, C.; Chapline, M. G.; Peng, S.; Cho, K.; Dai, H. Science 2000, 287, 622.
3. Tanahashi, M.; Matsuda, T. J Biomed Mater Res 1997, 34, 305.
4. Kikuchi, M.; Suetsugu, Y.; Tanaka, J.; Akao, M. J Mater Sci: Mater Med 1997, 8, 361.
5. Kasuga, T.; Fujikawa, H.; Abe, Y. J Mater Res 1999, 14, 418.
6. Li, W.-J.; Danielson, K. G.; Alexander, P. G.; Tuan, R. S. J Biomed Mater Res A 2003, 67, 1105.
7. Yoshimoto, H.; Shin, Y. M.; Terai, H.; Vacanti, J. P. Biomaterials 2003, 24, 2077.
8. Penumadu, D.; Dutta, A.; Pharr, G. M.; Files, B. J Mater Res 2003, 18, 1849.
9. Safadi, B.; Andrews, R.; Grulke, E. A. J Appl Polym Sci 2002, 84, 2660.
10. Sabba, Y.; Thomas, E. L. Macromolecules 2004, 37, 4815.
11. Choi, Y.-K.; Sugimoto, K.-I.; Song, S.-M.; Gotoh, Y.; Ohkoshi, Y.; Endo, M. Carbon 2005, 43, 2199.
12. Tamburri, E.; Orlanducci, S.; Terranova, M. L.; Valentini, F.; Palleschi, G.; Curulli, A.; Brunetti, F.; Passeri, D.; Alippi, A.; Rossi, M. Carbon 2005, 43, 1213.
13. Li, S.; Qin, Y.; Shi, J.; Guo, Z.-X.; Li, Y.; Zhu, D. Chem Mater 2005, 17, 130.
14. Shin, M.; Yoshimoto, H.; Vacanti, J.-P. Tissue Eng 2004, 10, 33.
15. Maeda, H.; Kasuga, T.; Nogami, M.; Hibino, Y.; Hata, K.-I.; Ueda, M. J Mater Res 2002, 17, 4.
16. Zhang, H.; Wang, B.; Li, H.; Jiang, Y.; Wang, J. Polym Int 2003, 52, 1493.